Supplementary Information

Surface-Assisted Assembly of Histidine-Rich Lipidated Peptide for Simultaneous Exfoliation of Graphite and Functionalization of Graphene Nanosheets

Lei Zhang, Yuebiao Sheng, Alireza Zehtab Yazdi, Kaveh Sarikhani, Feng Wang, Yunsheng Jiang, Juewen Liu, Tao Zheng, Wei Wang, Pingkai Ouyang* & P. Chen**

1. Methods

Dynamic Light Scattering Measurement: The hydrodynamic diameter size of exfoliated graphite was measured by dynamic light scattering (DLS) technology (Malvern Instruments, Malvern, UK). In general, 80 μL of exfoliated graphite solution by NP1 at pH 8.0 (six times dilution) and NP1-functionalized graphene co-assembled ellipticine was added into a quartz microcell with a 3 mm light path. The scattering intensity was collected at an angle of 173 °. The intensity-based size was analyzed by the Dispersion Technology software 5.0.

Cell Culture and Cytotoxicity Assay: The Chinese hamster ovary (CHO-K1) cells (ATCC, Manassas, USA) were cultured in F-12 Kaighn's modification medium (F-12K, HyClone Laboratories Inc., Utah, USA) supplemented with 10% fetal bovine serum (FBS, HyClone Laboratories Inc., Utah, USA). The cells were incubated at 37 °C in a humidified atmosphere containing 5% CO2.

CHO-K1 cells (8,000 cells/well) were plated in a 96-well plate. After 24 h incubation, the medium was removed and washed three-time with phosphate buffer saline (PBS, HyClone Laboratories Inc., Utah, USA). The NP1 (80 μM) and few-layered graphene (exfoliated by NP1 of 80 μM at pH 8.0) solution was diluted to different concentration (2.5, 5, 10 and 20 μM) with Opti-MEM (HyClone Laboratories Inc., Utah, USA). After that, 60 μL of each solution was added to the cells for 3 h incubation. Then 60 μL F-12K medium with 20% FBS was added in for another 24 h incubation. After that, all the solution was removed and washed three-time with PBS. Then 100 μL of Opti-MEM medium with CCK-8 reagent (HyClone Laboratories Inc., Utah, USA) was added to each well for another 3 h incubation. The plated was red to collect the absorbance of 570 nm by an FLUOstar OPTIMA microplate reader. Cell viability was calculated as the ratio of the cell treated over the non-treated one (negative control). We used the F-12K medium as the negative control.

2. UV-Vis Absorption Spectra of the Few-Layered Graphene Nanosheets

The peak of exfoliated graphite solution had blue shift to 267 nm compared with reported 268 nm.[1] It might be due to peptide adsorption onto the surface. The standard curve (Figure S1 B) was obtained by fitting the peak values at 267 nm in Figure S1 A. The R square is 0.999, and the fit equation is shown below:

$$\mathrm{Y} = -0.1313\mathrm{X} + 1.432$$

The exfoliation efficiency by using NP1 peptide at pH 4.0 was also quantified, and compared using the UV-Vis absorption, as shown in Figure S1 C, D. Similar trend was observed compare with the pH 8.0 case, for the graphite sample that was treated by NP1 is much higher than the samples treated by H16R8 (NP1 without stearic acid), Str-R8 (NP1 without histidine), histidine, imidazole, and water. The results indicated the importance of the stearic acid and histidine. And the contribution of histidine may be mainly due to the imidazole side chain.

It should be noted that literature reported peptide bonds in protein might contribute to the graphite exfoliation when using protein as the agent.[2] When we remove the histidine (Str-R8), the length of peptide changed, following the peptide

bonds changes, which might lead to the slight difference of the exfoliation efficiency. Our control experiment, histidine only indicates some exfolaiton, it could confirm the role of histidine. On the other hand, as we proposed that the histidine and arginine are used to bind to the graphite surface and help the graphite dispersion, respectively; the ratio between the histidine and arginine will definitely affect the exfoliation efficiency. For example, when we shorten the length of the histidine, the binding between the peptide and graphite will be limited and the work of adhesion will decrease, which might lead to lower exfoliation efficiency.

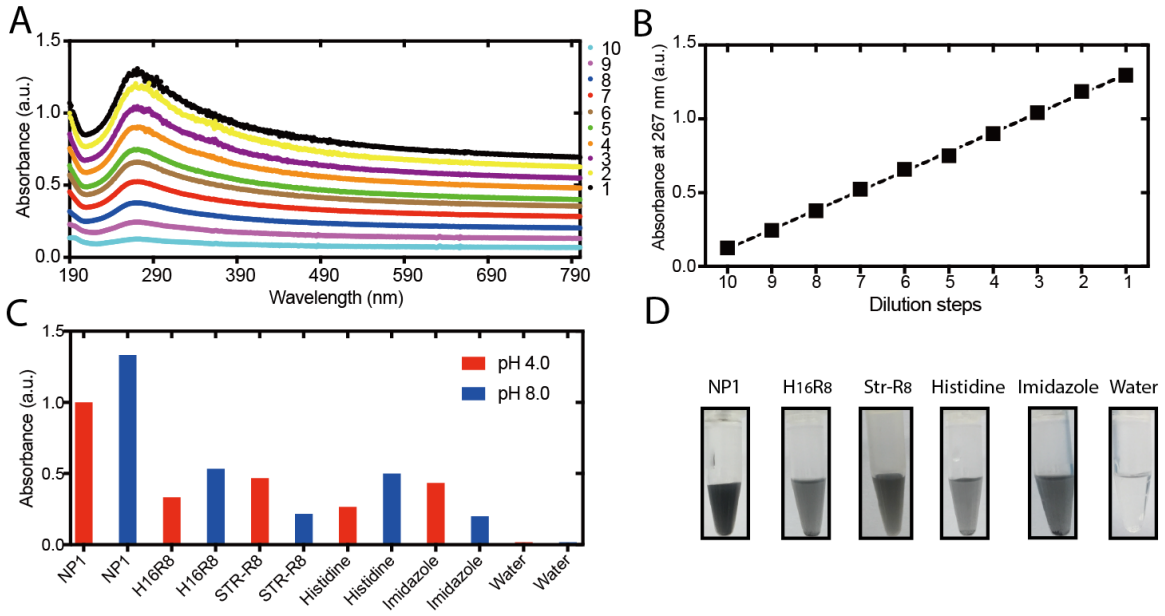

Figure S1. (A) UV–Vis absorption spectra of the exfoliated graphite by NP1 at pH 8.0 at different dilution steps and (B) the standard curve fitted by the values of the absorption peak at 267 nm in A. (C) UV-Vis absorptions of the solution in Figure 1 B and Figure S1 D (six times dilution). (D) Samples of exfoliation of graphite by NP1 and its individual segments at pH 4.0 (H16R8: without stearic acid, Str-R8: without histidine). The legend in A indicates the dilution factor from 1 to 10.

Table S1. Names and sequences of peptides used in the experiments.

Peptides Names	Sequences
NP1	Stearyl-HHHHHHHHHHHHHHHH-RRRRRRRR-NH_2
Str-R8	Stearyl-RRRRRRRR-NH_2
H16R8	Acetyl-HHHHHHHHHHHHHHHH-RRRRRRRR-NH_2
EAR16-I	Acetyl-AAEEAARRAAEEAARR-NH_2
EAR16-II	Acetyl-AEAEARARAEAEARAR-NH_2
EAR8-I	Acetyl-AAEEAARR-NH_2
EAR8-II	Acetyl-AEAEARAR-NH_2
ELR8-I	Acetyl-LLEELLRR-NH_2
ELR8-II	Acetyl-LELELRLR-NH_2

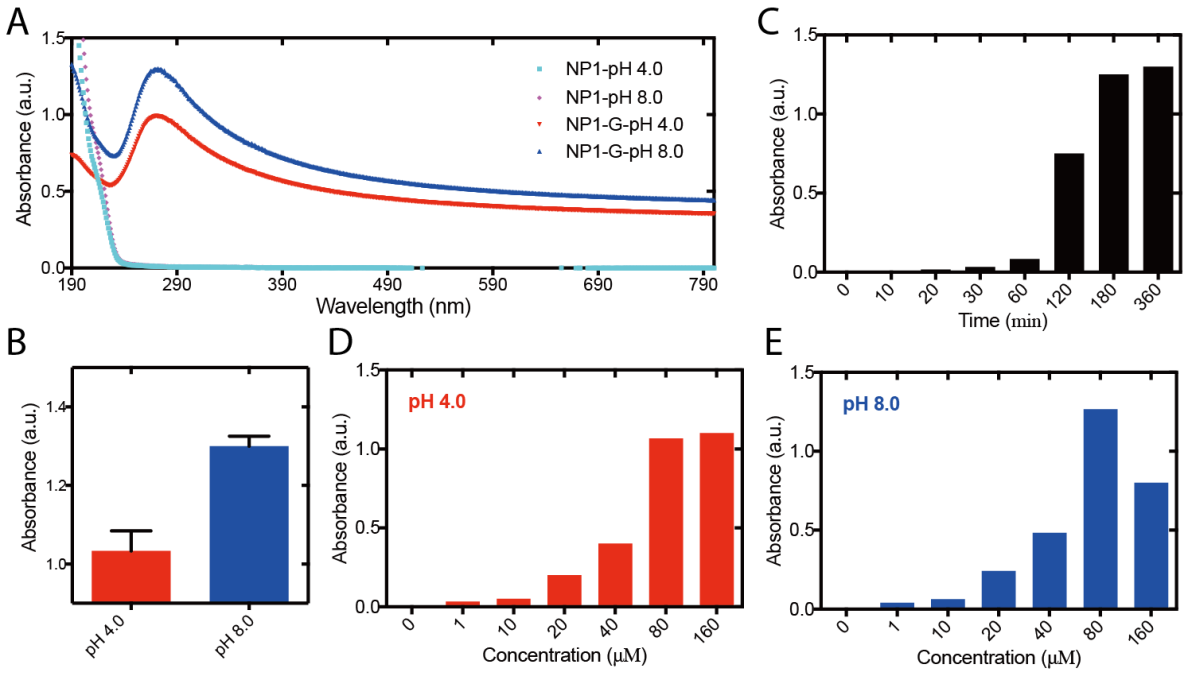

Figure S2. (A) UV-Vis absorptions of blank peptide at pH 4.0 and 8.0, and the exfoliated graphite by NP1 peptide at pH 4.0 and 8.0. (B) The statistic results (three repeat experiments) of the absorption of the exfoliated graphite by NP1 peptide at pH 4.0 and 8.0. Results are given as mean values ± SD, n = 3. (C) The effect of sonication time on graphite exfoliation using NP1 at pH 8.0. The effect of concentration of peptide on graphite exfoliation at (D) pH 4.0 and (E) 8.0. All the exfoliated samples were diluted six times for UV-Vis absorption measurements.

3. Dispersion Percentage of the Few-Layered Graphene Nanosheets

Table S2. The calculated graphite dispersion percentage (described in METHODS Section: Exfoliation protocol) using NP1 peptide and water at pH 4.0 and 8.0 for exfoliation.

1 mg Graphite	Water-pH 4.0	Water-pH 8.0	NP1-pH 4.0	NP1-pH 8.0
After sonication				
Transferring to tubes				
Remain after transferring				
Remain after 2nd centrifugation				
Totally remain weight (mg)	1.00 ± 0.06	1.03 ± 0.05	0.34 ± 0.03	0.18 ± 0.04
Dispersion percentage (%)	< 0	< 0	65.67 ± 3.06	82.01 ± 4.36

4. DLS Results of the Few-Layered Graphene Nanosheets

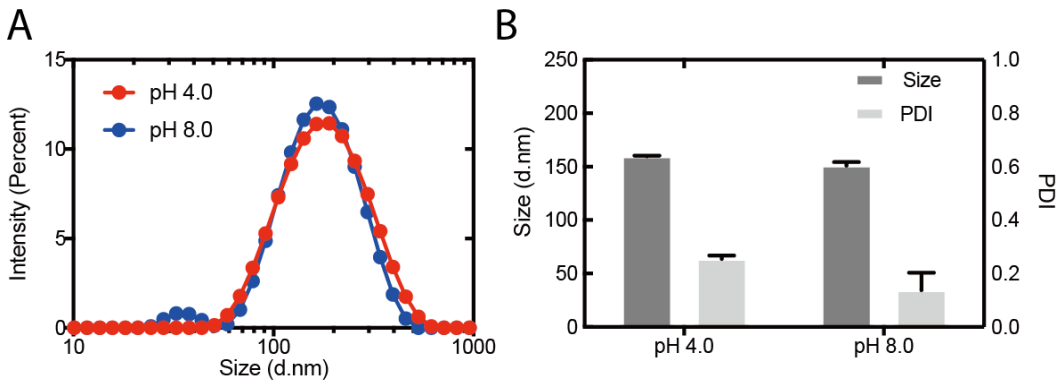

Figure S3. DLS results of the exfoliated graphite by NP1 peptide at pH 4.0 (A) and 8.0. (B) Sizes are stable for more than eight months with low PDI. Results are given as mean values ± SD, n = 3.

5. AFM and TEM Results of the Few-Layered Graphene Nanosheets

The formation of exfoliated graphite by NP1 at pH 4.0 was measured (Figure S4 A-C). Insert in Figure S4 B is the height information of a ~4 nm few-layered graphene nanosheet with roughness surface. Similar nanosheets were observed in Figure 1 C for the case of pH 8.0. The roughness surfaces with some bulges might be due to the coating of the peptide. It should be noted that the high-speed centrifugation (12,000 rpm) could remove some peptide coated on the few-layered graphene nanosheets surface *via* centrifugal force. In order to evaluate the number of graphene layers that correspond to 5 nm thickness, we conducted a literature survey, and realized that a wide range of thicknesses has been experimentally reported so far for single layer graphene sheets.[3] The thickness varies from 0.4 nm to 1.7 nm with majority ≥ 1 nm depending on the measurement method. For example, imaging mode and set point parameters in the AFM technique play a key role in measuring the thickness of graphene sheets. By changing the applied pressure throughout the course of measurement in AFM, the measured thickness could vary. The waviness of graphene sheets across the surface could also alter the final thickness of the graphene sheets. Assuming single layer graphene has a thickness of ~ 1 nm, we employed a peak-force tapping mode AFM from Bruker to measure the thickness of graphene flakes, and concluded more than 80 nanosheets that the majority of the flakes have 5 graphene layers (Figure S4 E, 1 H).

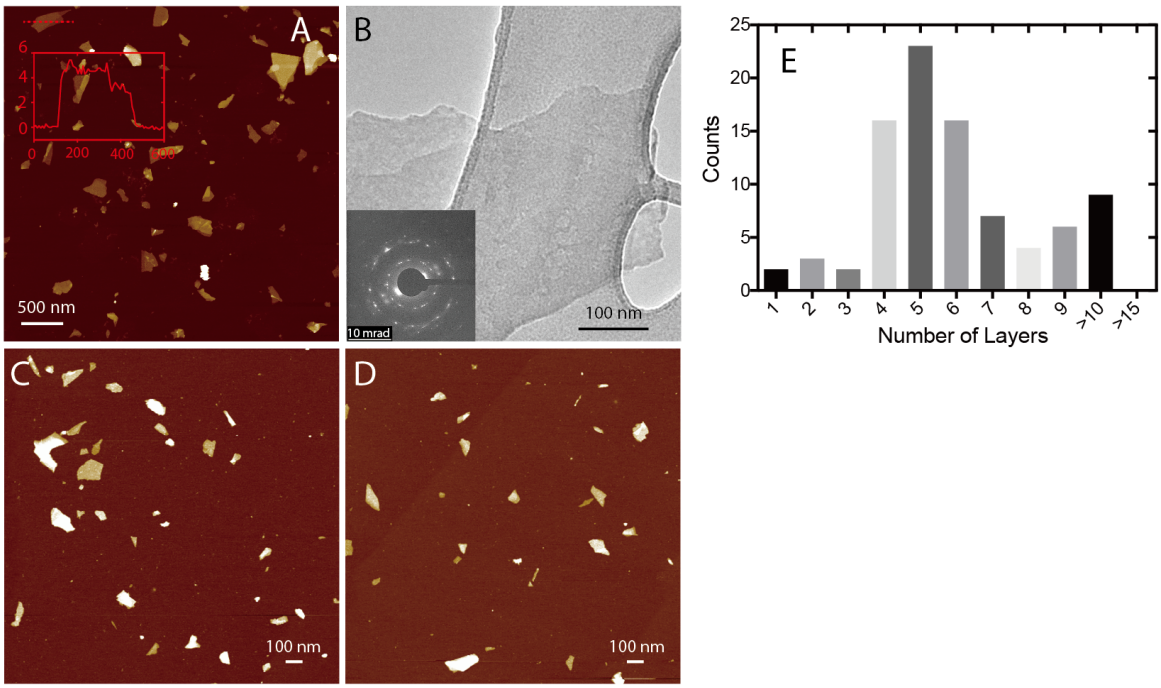

Figure S4. AFM images of exfoliated graphite by NP1 at (A, C) pH 4.0 and (D) pH 8.0. Inset in the AFM image is the height of the profiled few-layered graphene nanosheet by red line. (B) TEM image of exfoliated graphite by NP1 at pH 4.0. Inset in the TEM is the representative SEAD of the nanosheet. (E) Distributions of the numbers of the layer for over 80 nanosheets exfoliated by NP1 at pH 4.0.

6. Raman and XPS Results of the Few-Layered Graphene Nanosheets

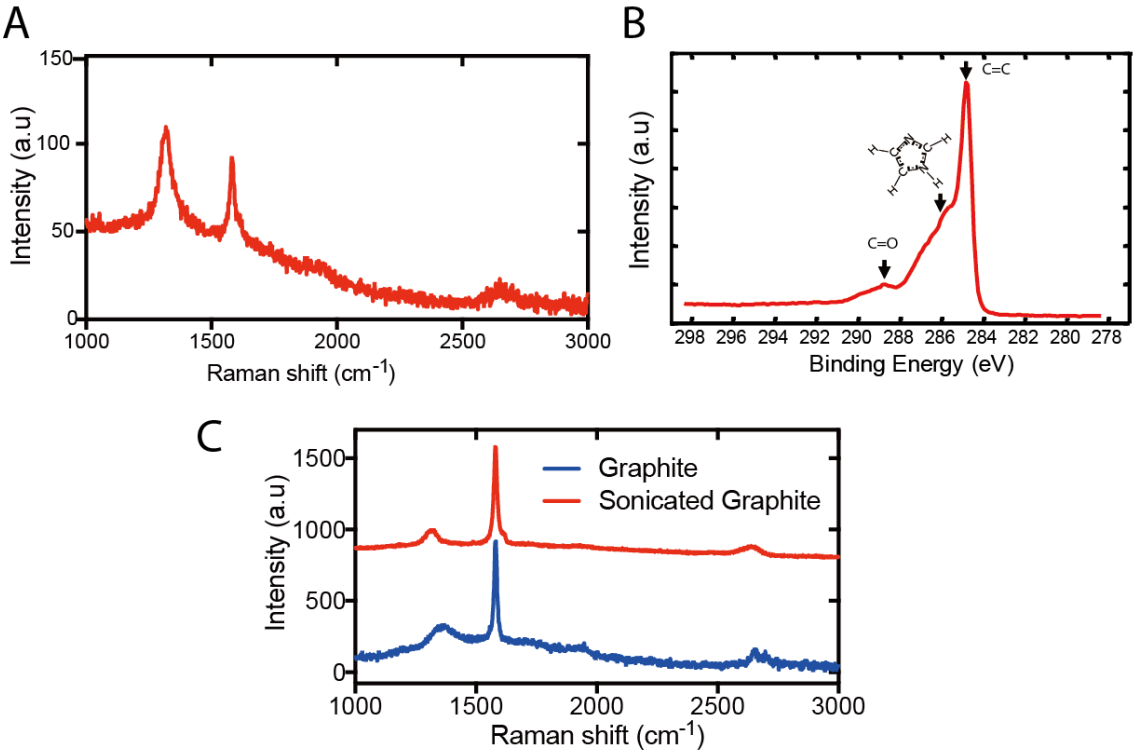

Figure S5. (A) Raman and (B) XPS results of the exfoliated graphite by NP1 at pH 4.0. (C) Raman results of the pristine and sonicated graphite in water for control.

7. AFM Morphologies of HOPG/Silica Wafer Surface Coated with NP1 Peptide

The 2D height images of Figure S6 A, B were shown in Figure 2 D, G, respectively. The parallel stripes were also observed in different directions. (Figure 2 D-F) Clearly boundaries occurred in the blank HOPG surfaces, as well as the peptide coated ones. The height and size of single parallel stripe and the porous microstructures of assembled NP1 were measured and shown in Figure 2 D, E, G.

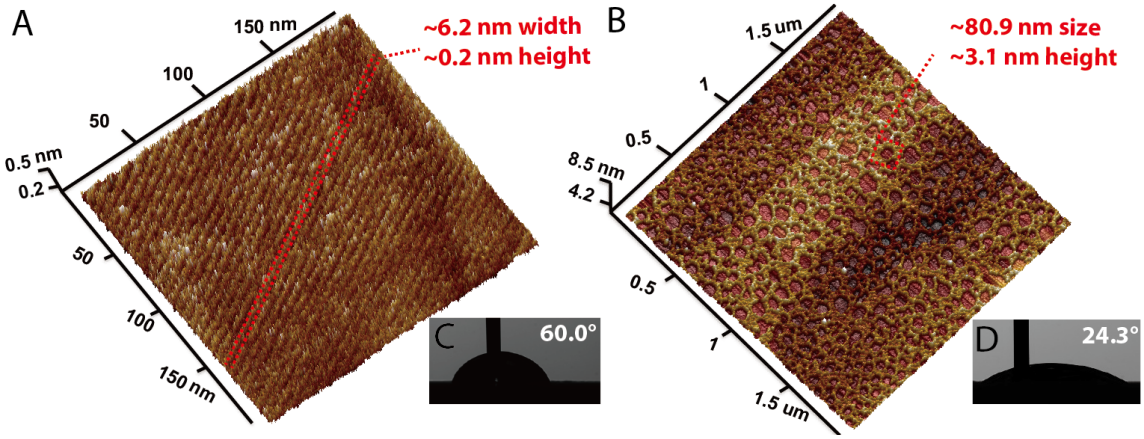

Figure S6. 3D AFM images of the coated NP1 peptide on the HOPG surface at (A) pH 4.0 and (B) 8.0. (C) and (D) are the corresponding contact angles.

It should be noted that it was hard to observe the similar ordered peptide structure on the few-layered graphene nanosheet surface. The possibilities of interpretation might be that the bath sonication could affect the ordering surface-assisted assembly behavior of NP1 peptide. In addition, the high-speed centrifugation could remove some of the coated NP1 *via* centrifugal force.

As shown in Figure S7 E-J, more aggregation was observed for the NP1 at pH 8.0 coated silica wafer surface than the pH 4.0 case. It might be due to the deprotonated NP1 at pH 8.0 could contribute the hydrogen bonding, which could drive the assembly and aggregation of peptide.

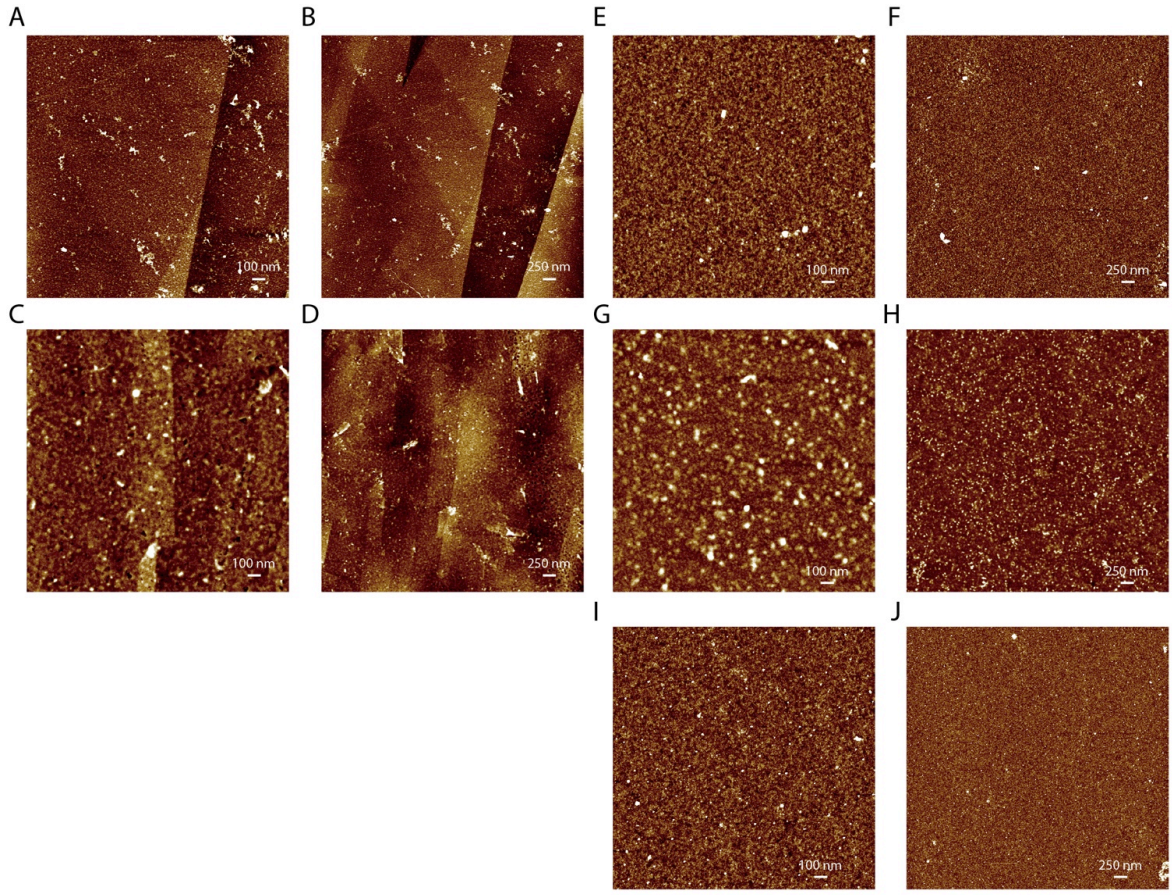

Figure S7. AFM images of the coated NP1 peptide on HOPG surface at (A, B) pH 4.0 and (C, D) 8.0. AFM images of the coated NP1 peptide at (E, F) pH 4.0, (G, H) 8.0 on silica wafer surface and (I, J) blank silica wafer surface. The incubation time of 60 min was used for pH 4.0 and 30 min for pH 8.0.

8. Contact Angle Measurements and the Work of Adhesion

The water contact angles and surface energy calculations of the peptide solution coated on HOPG surface showed higher hydrophilicity of NP1 peptide at pH 8.0 as a result of orientation of the charged functional groups on the outermost side of peptide coating (the side in touch with water in contact angle measurement). Having the charge side of peptide layer at pH 8.0 on the waterside, one could conclude that the other side of peptide with a lower surface energy to be on the inner side and contact with HOPG surface. It means that the interaction and binding between NP1 peptide at pH 8.0 and HOPG occurs between hydrophobic tail and histidine block of NP1 peptide and the graphitic surface (the side with lower surface energy). The lower contact angle for the deprotonated peptide at pH 8.0 in comparison with pH 4.0 confirms this hypothesis. Another confirmation for change in orientation of peptide molecules on substrate is the contact angle measurements of the silicon wafer (hydrophilic surface) that is coated with peptide. The results showed an opposite trend compared with HOPG; the contact angles for pH 4.0 and 8.0 are the opposite of those for HOPG surface. The reason might be because of orientation of the charged block in the inner side, which is contact with the hydrophilic silicon substrate. Consequently, at pH 8.0 the presence of the charged arginine block on the substrate leads to the creation of a hydrophobic surface on the outermost side of the substrate. Therefore, the surface energy and contact angle results obtained from coated peptide on silicon wafer represented the very side of peptide chain in contact with hydrophobic surfaces such as graphene, graphite, and HOPG. The hydrophobic tail with strong van der Waals and π-π interaction with HOPG/graphite surface would be in contact with the surface, and the charged side oriented toward outside (it was water phase while the coating happens) as reported in the study of monolayer surfaces[4]. In pH 4.0, the repulsive forces prevented the uniform and cooperative alignment of the hydrophobic tail and charged hydrophilic side. Therefore, the coexistence of hydrophobic patches

among hydrophilic charge patches minimized the effectiveness of the charges patches in wetting properties of coated peptide.[5] The calculated work of adhesion between peptide and HOPG in water were obtained from contact angle measurement of the peptide-coated silicon wafer samples.

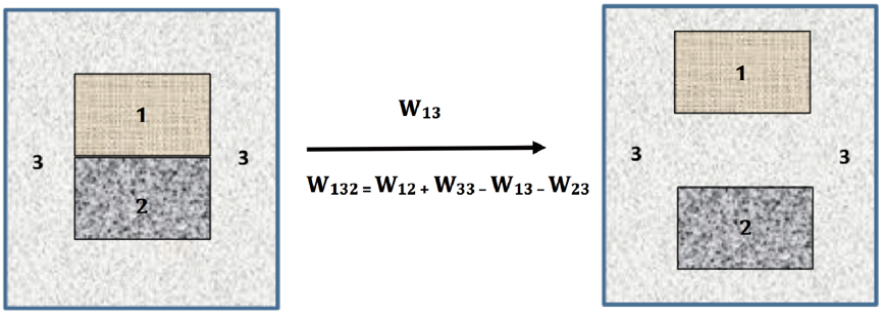

Figure S8. The schematic representation of work of adhesion definition between two components in a third medium where the graphene surface is denoted by number 1, peptide by number 2, and the medium (water) by number 3.

9. Molecular Dynamics Simulations

Due to the different protonated/deprotonated states of the histidine residues, the adsorption of NP1 peptide shows different behaviors. Under neutral condition, one peptide chain (Figure 4 D) gradually approaches the HOPG surface and finally deposits on the surface at ~ 3.9 ns till the end of the simulation; while the protonated peptide under acidic condition (Figure 4 A) finally adsorbs on the HOPG surface at ~20.8 ns. When histidine residues of the peptide are protonated, both histidine and arginine residues are positively charged, a turn happens to screen the part of the electrostatic repulsive interactions and the peptide molecules form ordered structure on the HOPG surface. While as the most of the positively charged side-chains of the peptide point to the solvent, the strong electrostatic repulsive interactions hinder the formation of a second layer of peptide. In contrast, when histidine residues of the NP1 peptide are deprotonated, only arginine residues are positively charged, but both the histidine residues and the stearic acid tail are highly hydrophobic, which makes the peptide adsorbs on the HOPG surface quickly; due to the lack of strong electrostatic repulsive interactions, the peptide molecules can stack multilayers (or compact) structure on the surface and form specific patterns as the result of the symmetry of the graphite surface.

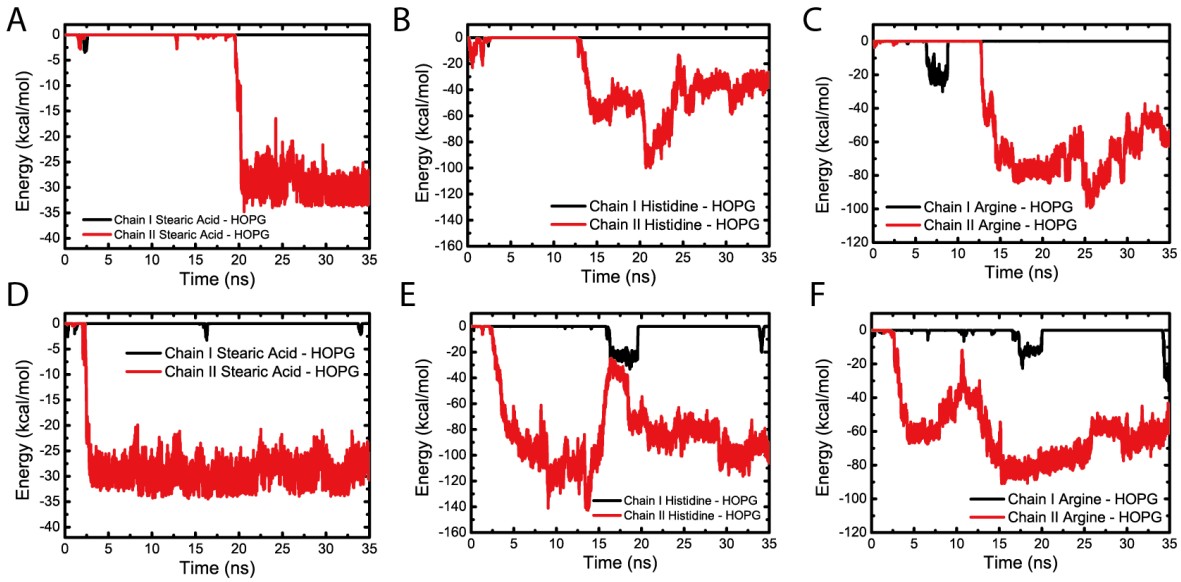

Figure S9. Time evolution plots of (A) the energy of stearic acid in each peptide molecule with HOPG surface, (B) the energy of histidine residues in each peptide molecule with HOPG surface, and (C) the energy of arginine residues in each peptide molecule with HOPG surface under acidic condition. Corresponding plots under neutral condition are showed in D to F.

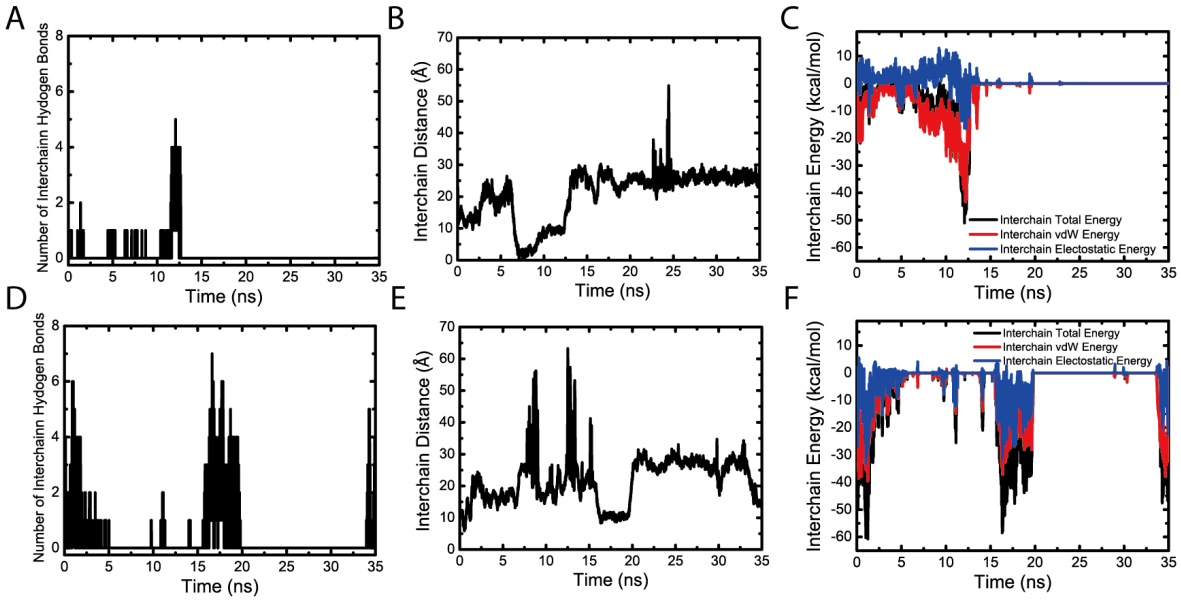

Figure S10. Time evolution plots of (A) the number of interchain hydrogen bonds, (B) the NP1 interchain distance, and (C) the interchain energies under acidic condition. Corresponding plots under neutral condition are showed in D to F.

Table S3. Number of interchain hydrogen bonds with different lasting time during the simulation. It should be noted that although interchain hydrogen bonds can be observed during the adsorption process, their lasting time is very short and these hydrogen bonds form and break frequently, indicating that the hydrogen bonding is very weak comparing to other interactions, and the number of hydrogen bonds in the table only reflects the trend of hydrogen bonding variation.

Condition	Lasting Time (ps)	Number
Acidic	≤10	86
	10~50	20
	>50	9
Neutral	≤10	320
	10~50	95
	>50	9

References

1. Z. Z. Sun, Z. Yan, J. Yao, E. Beitler, Y. Zhu and J. M. Tour, *Nature*, 2010, 468, 549-552.
2. G. J. Guan, S. Y. Zhang, S. H. Liu, Y. Q. Cai, M. Low, C. P. Teng, I. Y. Phang, Y. Cheng, K. L. Duei, B. M. Srinivasan, Y. G. Zheng, Y. W. Zhang and M. Y. Han, *J Am Chem Soc*, 2015, 137, 6152-6155.
3. C. J. Shearer, A. D. Slattery, A. J. Stapleton, J. G. Shapter and C. T. Gibson, *Nanotechnology*, 2016, 27, 125704.
4. Y. Chen, C. Helm and J. Israelachvili, *The Journal of Physical Chemistry*, 1991, 95, 10736-10747.
5. S. Granick and S. C. Bae, *Science*, 2008, 322, 1477-1478.